

## Surface Raman Spectroscopy of the Interface of Tris-(8-hydroxyquinoline) Aluminum with Mg

Robert J. Davis and Jeanne E. Pemberton\*

Department of Chemistry, University of Arizona, 1306 E. University Boulevard,  
Tucson Arizona 85721

Received October 10, 2008

**Abstract:** Surface Raman spectroscopy in ultrahigh vacuum is used to interrogate interfaces formed between tris-(8-hydroxyquinoline) aluminum ( $\text{Alq}_3$ ) and vapor-deposited Mg. The Raman spectral results for deposition of Mg mass thicknesses between 5 and 20 Å indicate formation of a complex interfacial region composed primarily of Mg– $\text{Alq}_3$  adducts and small-grained amorphous or nanocrystalline graphite, the presence of which may have a significant effect on the electronic properties of this metal–organic interface. The observed shifts in  $\nu_{\text{ring}}$ ,  $\nu(\text{C–N})$ ,  $\nu(\text{Al–N})$ , and  $\nu(\text{Al–O})$  modes along with the appearance of  $\nu(\text{Mg–C})$  and  $\nu(\text{Mg–O})$  modes suggest a structure for the Mg– $\text{Alq}_3$  adduct in which Mg is bound to the O and C atoms of  $\text{Alq}_3$ . In addition, several intense, broad modes are observed that are consistent with partial graphitization of the  $\text{Alq}_3$  film.

### Introduction

Following its first demonstration as an efficient electroluminescent material over 20 years ago, tris-8-hydroxyquinoline aluminum ( $\text{Alq}_3$ ) has become a common electron transport and emissive layer in organic light emitting diodes (OLEDs).<sup>1</sup> Efficiency in these devices is governed largely by the rates for the transfer of charge across interfaces of dissimilar materials such as the organic semiconductors used as the hole and electron transport layers and the inorganic materials commonly used as cathodes and anodes. One critical interface in such devices is that involving the organic electron transport layer and the metallic cathode. Low work function metals are typically used as cathode materials in an effort to minimize the electron injection barrier at this interface by matching the Fermi level of the metal to the electron affinity of the electron transport layer. In studies of electroluminescent efficiency as a function of cathode metal in devices based on  $\text{Alq}_3$ , the highest efficiencies have been reported for devices using a Mg cathode when compared to other low work function metals such as Ag, Al, Ca, or Li.<sup>2</sup> The high rate of electron injection at the Mg/ $\text{Alq}_3$  interface has led to its widespread use in OLEDs and has spurred considerable interest in understanding the electronic and chemical structure of this system.

The formation of charge transfer complexes between metals and  $\text{Alq}_3$  are often invoked to explain spectroscopic changes in  $\text{Alq}_3$  films upon deposition of low work function metals.<sup>3–16</sup>

In addition, the presence of gap states between the Fermi and vacuum levels at the interface has been claimed for the Mg– $\text{Alq}_3$  interface based on UPS studies, whereas shifts in the  $\text{Alq}_3$  N, O, and C 1s electrons to lower binding energies, along with the appearance of N and O 1s components at higher binding energy, have been reported in XPS studies of this interface.<sup>6,7,10</sup> These findings suggest formation of new species at the Mg– $\text{Alq}_3$  interface resulting from chemical reaction of the deposited Mg with  $\text{Alq}_3$ . Shen et al. interpreted changes in the XPS binding energies of the N 1s, O 1s, and Al 2p electrons as evidence for a Mg– $\text{Alq}_3$  adduct in which Mg is bound to the 8-hydroxyquinolate (8-HQ) ligand of one  $\text{Alq}_3$  through both C and N atoms with additional binding to an O atom of a neighboring 8-HQ.<sup>6</sup> This structure stands in contrast to that proposed for reaction of Al with  $\text{Alq}_3$  on the basis of UPS/XPS,<sup>3,4,6,8</sup> Raman,<sup>17</sup> and theoretical studies.<sup>9,11</sup> For this system, it has been concluded that Al is bound only to the O atom of the 8-HQ ligand. A similar structure to the Al product has also been proposed for Ca.

Theoretical studies of the reaction of Mg with  $\text{Alq}_3$  have resulted in conflicting structures for the resulting Mg– $\text{Alq}_3$  adduct.<sup>9,12–14</sup> Zhang et al. have proposed that Mg bonds to the

- (1) Tang, C. W.; Vanslyke, S. A. *Appl. Phys. Lett.* **1987**, *51*, 913.
- (2) Stossel, M.; Staudigel, J.; Steuber, F.; Simmerer, J.; Winnacker, A. *Appl. Phys. A: Mater. Sci. Process.* **1999**, *68*, 387.
- (3) Choong, V. E.; Mason, M. G.; Tang, C. W.; Gao, Y. *Appl. Phys. Lett.* **1998**, *72*, 2689.
- (4) Le, Q. T.; Yan, L.; Gao, Y.; Mason, M. G.; Giesen, D. J.; Tang, C. W. *J. Appl. Phys.* **2000**, *87*, 375.
- (5) Rajagopal, A.; Kahn, A. *J. Appl. Phys.* **1998**, *84*, 355.
- (6) Shen, C.; Kahn, A.; Schwartz, J. *J. Appl. Phys.* **2001**, *89*, 449.
- (7) Turak, A.; Grozea, D.; Feng, X. D.; Lu, Z. H.; Aziz, H.; Hor, A. M. *Appl. Phys. Lett.* **2002**, *81*, 766.

- (8) Yan, L.; Mason, M. G.; Tang, C. W.; Gao, Y. L. *Appl. Surf. Sci.* **2001**, *175*, 412.
- (9) Zhang, R. Q.; Lu, W. C.; Lee, C. S.; Hung, L. S.; Lee, S. T. *J. Chem. Phys.* **2002**, *116*, 8827.
- (10) Shen, C.; Hill, I. G.; Kahn, A.; Schwartz, J. *J. Am. Chem. Soc.* **2000**, *122*, 5391.
- (11) Curioni, A.; Andreoni, W. *J. Am. Chem. Soc.* **1999**, *121*, 8216.
- (12) Zhang, R. Q.; Hou, X. Y.; Lee, S. T. *Appl. Phys. Lett.* **1999**, *74*, 1612.
- (13) Meloni, S.; Palma, A.; Schwartz, J.; Kahn, A.; Car, R. *J. Am. Chem. Soc.* **2003**, *125*, 7808.
- (14) Meloni, S.; Palma, A.; Kahn, A.; Schwartz, J.; Car, R. *J. Appl. Phys.* **2005**, *98*, 23707.
- (15) Takeuchi, K.; Yanagisawa, S.; Morikawa, Y. *Sci. Tech. Adv. Mat.* **2007**, *8*, 191.
- (16) He, P.; Au, F. C. K.; Wang, Y. M.; Cheng, L. F.; Lee, C. S.; Lee, S. T. *Appl. Phys. Lett.* **2000**, *76*, 1422.
- (17) Davis, R. J.; Pemberton, J. E. *J. Phys. Chem. C* **2008**, *112*, 4364.

O atom of Alq<sub>3</sub> to form a 1:1 Alq<sub>3</sub>–Mg complex.<sup>9</sup> However, in addition to Mg–O bonding as observed for other metals (e.g., Al<sup>9,11</sup> and Ca<sup>11,15</sup>), formation of Mg–C bonds must also be considered because stable Mg–C bonds in Mg–aromatic systems are well documented.<sup>18–23</sup> Starting with this premise, DFT calculations of Meloni et al. predict a stable 1:2 Mg–Alq<sub>3</sub> complex for a crystalline Alq<sub>3</sub> matrix in which Mg is bound through one O and two C atoms of one Alq<sub>3</sub> with additional coordination to an O atom of a neighboring Alq<sub>3</sub>.<sup>13,14</sup> As noted by these authors, this proposed structure agrees with previously reported XPS shifts in the O and N 1s core levels for the Mg–Alq<sub>3</sub> interface. Unfortunately, the breadth of the C 1s peak does not allow direct confirmation of Mg–C bond formation.<sup>6,7,10</sup>

The bonding in the Mg–Alq<sub>3</sub> complex proposed by Meloni et al. indicates that a more expansive view of potential reactivity and stoichiometry is required to understand these complex interfaces. Unfortunately, XPS of metal–Alq<sub>3</sub> systems is not particularly sensitive to changes in carbon bonding due to the large number of carbon atoms present in different chemical environments in Alq<sub>3</sub>. Thus, methods are needed that are better suited for observing changes in carbon bonding. The investigation described in this report adds the first Raman spectroscopy results to the growing body of work characterizing the Mg/Alq<sub>3</sub> interface.

## Experimental Section

Thin films were prepared and characterized in a custom-built ultrahigh vacuum (UHV) chamber with a base pressure of  $7 \times 10^{-11}$  Torr described previously.<sup>17</sup> 8-Hydroxyquinoline, aluminum salt (Alq<sub>3</sub>, Aldrich, 99.995%), and Mg turnings (Alpha Aesar, 99.98%) were degassed at 525 and 700–900 K, respectively, at  $10^{-9}$  Torr for 6 h prior to deposition. A chemically polished,<sup>24,25</sup> 1.25 cm diameter Ag disk (Alfa Aesar, 99.999%) was used as the underlying substrate for all experiments. Amorphous or  $\alpha$ -Alq<sub>3</sub> films<sup>26</sup> were prepared on substrates held at 300 K. Mg was deposited onto the Alq<sub>3</sub>–Ag sample held at  $\sim 90$  K from Al<sub>2</sub>O<sub>3</sub>-coated W/Ta crucibles to ensure a sticking coefficient of unity. Film deposition was monitored differentially using a multilayer deposition monitor (Maxtek TM-400) and a gold-coated quartz sensor crystal (Maxtek SC-101). The sensor was held at room temperature for Alq<sub>3</sub> deposition but cooled with liquid N<sub>2</sub> during metal deposition; reported values of coverage represent mass thicknesses of the metal assuming bulk density.

Raman spectra were acquired with 20 mW of 514.5 nm radiation from a Coherent Innova 350C Ar<sup>+</sup> laser on a system described previously.<sup>17</sup> Typical spectral integration times varied from 10–30 min. Peak fitting of Raman spectra was accomplished using 100% Gaussian peaks. Peaks at frequencies associated with intense Alq<sub>3</sub> modes were fit using peak frequencies ( $\pm 5$  cm<sup>-1</sup>) and relative intensities ( $\pm 10\%$ ) determined by Halls and Aroca<sup>26</sup> with fwhm values of 15 cm<sup>-1</sup> ( $\pm 10$  cm<sup>-1</sup>). Modes associated with graphitic carbon were fit using five broad bands using peak frequencies ( $\pm 10$

cm<sup>-1</sup>), relative intensities ( $\pm 50\%$ ), and fwhm ( $\pm 50\%$ ) described by Ferrari and Robertson.<sup>27</sup> Additional spectral features were fit with broad bands that were allowed to vary in frequency by  $\pm 10$  cm<sup>-1</sup>, in fwhm by  $\pm 10$  cm<sup>-1</sup>, and intensity by  $\pm 50\%$ .

## Results and Discussion

To date, only a handful of studies have interrogated metal–Alq<sub>3</sub> interfacial chemistry by vibrational spectroscopy,<sup>17,28–30</sup> and no analyses have been reported for the Mg/Alq<sub>3</sub> interface. Sakurai et al. examined K–Alq<sub>3</sub> complexes by IR and Raman spectroscopy and observed formation of an ionic complex in which, following a charge transfer reaction, Alq<sub>3</sub><sup>-</sup> is present associated with K<sup>+</sup> counterions.<sup>31</sup> In a previous report from this laboratory, Raman spectroscopy of the Al–Alq<sub>3</sub> system suggested formation of an Al–Alq<sub>3</sub> complex with Al covalently bound to two O atoms of 8-HQ.<sup>17</sup> Significantly, Raman spectral modes of graphitic carbon were also observed for the first time in this system indicating partial decomposition of Alq<sub>3</sub> upon Al deposition.

Collectively, these results speak to the complexity and reactivity of these interfaces and the challenges inherent in their characterization. Moreover, oxide formation by low work function metals has been shown to reduce performance in devices utilizing metal/Alq<sub>3</sub> contacts,<sup>31,32</sup> thereby requiring the use of ultrahigh vacuum environments to prevent such extrinsic interface reactions during characterization. The study reported here combines a UHV platform, which allows environmental control of these reactive systems, with Raman spectroscopy, with its inherent high specificity and sensitivity to changes in structure and bonding at metal–organic interfaces, allowing for the first time direct monitoring of the chemistry of the Mg/Alq<sub>3</sub> interface.

The Raman spectrum of a 150 Å thick Alq<sub>3</sub> film deposited onto a chemically polished Ag substrate held at 90 K is shown in part a of Figure 1. The frequency of all vibrational modes observed agree with those previously reported for amorphous thin films of Alq<sub>3</sub>.<sup>17,26</sup> The bands at 1595 and 1394 cm<sup>-1</sup> correspond to the  $\nu_{\text{ring}}$  and [ $\nu_{\text{ring}} + \delta(\text{C–H})$ ] modes of the 8-hydroxyquinolate (8-HQ) ligand. Lower-frequency bands are attributed to the  $\nu_{\text{ring}}$  mode at 757 cm<sup>-1</sup>, the [ $\nu(\text{Al–O}) + \nu(\text{Al–N}) + \delta_{\text{ring}}$ ] combination modes at 647 and 543 cm<sup>-1</sup>, the [ $\delta_{\text{ring}} + \nu(\text{Al–O})$ ] combination mode at 525 cm<sup>-1</sup>, and a  $\delta_{\text{ring}}$  mode at 504 cm<sup>-1</sup>. Preservation of peak frequencies and intensity ratios compared to the calculated spectrum reported by Halls and Aroca<sup>26</sup> for amorphous Alq<sub>3</sub> confirms that the Alq<sub>3</sub> structure is retained upon its vapor deposition onto the Ag substrate and that no reaction occurs between Alq<sub>3</sub> and Ag as noted previously.<sup>17</sup>

Film deposition conditions and the frequencies of observed vibrational bands indicate a generally amorphous thin film of *mer*-Alq<sub>3</sub> isomers<sup>29,30,33</sup> with a preference for formation of the  $\alpha$ -Alq<sub>3</sub> crystal phase.<sup>26,33</sup> Similar amorphous thin films deposited

- (18) Bogdanovic, B. *Acc. Chem. Res.* **1988**, *21*, 261.  
 (19) Mason, M. G.; Tang, C. W.; Hung, L.-S.; Raychaudhuri, P.; Madathil, J.; Giesen, D. J.; Yan, L.; Le, Q. T.; Gao, Y.; Lee, S.-T.; Liao, L. S.; Cheng, L. F.; Salaneck, W. R.; dos Santos, D. A.; Brédas, J. L. *J. Appl. Phys.* **2001**, *89*, 2756–2765.  
 (20) Engelhardt, L. M.; Harvey, S.; Raston, C. L.; White, A. H. *J. Organomet. Chem.* **1988**, *341*, 39.  
 (21) Brooks, W. M.; Raston, C. L.; Sue, R. E. *Organometallics* **1991**, *10*, 2098.  
 (22) Stegmann, R.; Frenking, G. *Can. J. Chem.* **1996**, *74*, 801.  
 (23) Aleksanyan, V. T.; Garbuzova, L. A.; Gavrilenko, V. V.; Zakharkin, L. I. *J. Organomet. Chem.* **1977**, *129*, 139.  
 (24) Smolinski, S.; Zelenay, P.; Sobkowski, J. *J. Electroanal. Chem.* **1998**, *442*, 41.  
 (25) Tiani, D. J.; Pemberton, J. E. *Langmuir* **2003**, *19*, 6422.  
 (26) Halls, M. D.; Aroca, R. *Can. J. Chem.* **1998**, *76*, 1730.

- (27) Ferrari, A. C.; Robertson, J. *Phys. Rev. B* **2000**, *61*, 14095.  
 (28) Sakurai, Y.; Salvan, G.; Hosoi, Y.; Ishii, H.; Ouchi, Y.; Seki, K.; Kampen, T. U.; Zahn, D. R. T. *Appl. Surf. Sci.* **2002**, *190*, 382.  
 (29) Sakurai, Y.; Hosoi, Y.; Ishii, H.; Ouchi, Y.; Salvan, G.; Kobitski, A.; Kampen, T. U.; Zahn, D. R. T.; Seki, K. *J. Appl. Phys.* **2004**, *96*, 5534.  
 (30) Sakurai, Y.; Yokoyama, T.; Hosoi, Y.; Ishii, H.; Ouchi, Y.; Salvan, G.; Kobitski, A.; Kampen, T. U.; Zahn, D. R. T.; Seki, K. *Syn. Met.* **2005**, *154*, 161.  
 (31) Shen, C. F.; Hill, I. G.; Kahn, A. *Adv. Mater.* **1999**, *11*, 1523.  
 (32) Broms, P.; Birgersson, J.; Salaneck, W. R. *Syn. Metals* **1997**, *88*, 255.  
 (33) Brinkmann, M.; Gadret, G.; Muccini, M.; Taliani, C.; Masciocchi, N.; Sironi, A. *J. Am. Chem. Soc.* **2000**, *122*, 5147.

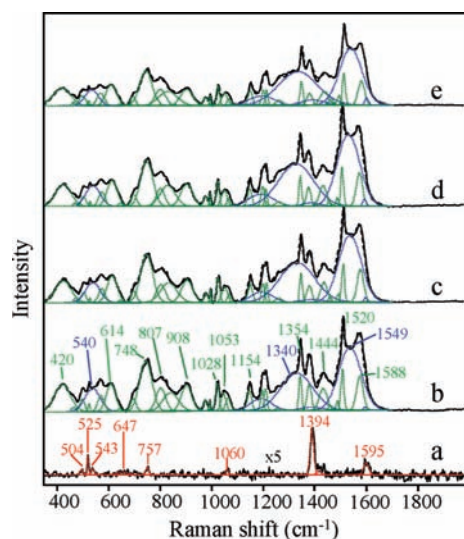


**Figure 1.** Peak fits of Raman spectra of a) pristine 150 Å Alq<sub>3</sub> film on Ag and after deposition of mass thicknesses of b) 5, c) 10, d) 15, and e) 20 Å Mg. Raman spectrum (black —), overall fit envelope (black - - -), Alq<sub>3</sub> modes (red - - -), Mg–Alq<sub>3</sub> reaction product modes (green - - -), and graphitic carbon modes (blue - - -).

at 300 K and cooled to 4.2 K have been shown by X-ray diffraction to generally retain their amorphous character but to slightly order.<sup>33</sup> Thus, cooling of these films to 90 K for the Raman spectral studies reported here should have minimal effect on film structure.

Parts b–e of Figure 1 show Raman spectra at 90 K after deposition of 5 to 20 Å of Mg. Mg has a low atomic ionization potential that supports electron transfer to the conjugated 8-HQ ring and is widely considered to undergo a chemical reaction with the organic layer.<sup>3–6,8–10,12–14,16</sup> Despite the expectation based on past work of chemical reaction at this interface, the potential for surface enhanced Raman scattering (SERS) upon formation of metallic Mg clusters at the interface must be considered when interpreting the Raman spectral changes observed for this system. Previous Raman spectral studies from this laboratory of Ag postdeposition onto Alq<sub>3</sub> films have documented such a SERS effect that leads to enhancement of native Raman modes and the activation of certain IR-active modes.<sup>17,26</sup> In the case of Mg postdeposition, however, the peak frequencies, shapes, and intensity ratios of the new spectral bands in parts b–e of Figure 1 do not match well with the known vibrational modes<sup>26</sup> that are enhanced at the nonreactive Ag–Alq<sub>3</sub> interface.<sup>17</sup> Thus, SERS as a general explanation for the changes observed upon Mg deposition is rejected leading to the conclusion of chemical reaction at the interface.

Even with deposition of only 5 Å of Mg (part b of Figure 1), significant spectral changes are observed relative to the pristine Alq<sub>3</sub> film that indicate substantive structural changes to the Alq<sub>3</sub> film upon contact with Mg. To elucidate the spectral contributions from Mg–Alq<sub>3</sub> reaction products, modes from unreacted Alq<sub>3</sub>, and modes from other species formed at the metal–organic interface, these spectral results were subjected to peak fitting. Whereas the complexity of the observed spectra and the presence of overlapping vibrational modes prevent precise determination of peak frequencies and intensities, general trends in the peak fits provide considerable insight into structural changes occurring at the metal–organic interface that have not been identifiable heretofore. Assignments for the major product modes identified by peak fitting are presented in Table 1; complete assignment

**Table 1.** Raman Peak Frequencies and Assignments for Pristine Alq<sub>3</sub> and after Deposition of 20 Å of Mg

Raman Shift (cm <sup>-1</sup> )			Mode Assignments <sup>a</sup>
literature Alq <sub>3</sub> <sup>31</sup>	150 Å Alq <sub>3</sub>	20 Å Mg on Alq <sub>3</sub>	
1595	1595	1610	$\nu_{\text{ring}} + \nu_{\text{ring}}$ graphite D'-band
		1588	$\nu_{\text{ring}}$
		1549	graphite G-band
		1400	graphite G-band
1394	1394	1390	$\nu_{\text{ring}} + \delta(\text{C-H})$
		1340	graphite D-band
1335		1265	$\nu_{\text{ring}} + \nu(\text{C-O}) + \delta(\text{C-H})$
1230		1205, 1218	$\nu(\text{C-N}) + \delta(\text{C-H})$
		1200	graphite D-band
1117		1070	$\nu(\text{C-O}) + \delta(\text{C-H})$
		999	$[\nu(\text{Al-N}) + \delta(\text{C-H})_{\text{wag}}]_{\text{Mg adduct}}$
757	757	748	$\nu_{\text{ring}}$
		698	$[\nu(\text{Al-O}) + \delta(\text{Al-O-C})]_{\text{Mg adduct}}$
647	647	645	$\nu(\text{Al-O}) + \nu(\text{Al-N}) + \delta_{\text{ring}}$
		614	$\nu(\text{Mg-O})$
577		574	$\delta_{\text{ring}} + \delta(\text{Al-O-C})$
541	543		$\nu(\text{Al-O}) + \nu(\text{Al-N}) + \delta_{\text{ring}}$
		540	graphite $\delta_{\text{ring}}$
525	525	525	$\delta_{\text{ring}} + \nu(\text{Al-O})$
504	504	497	$\delta_{\text{ring}}$
		420	$\nu(\text{Mg-C})$

<sup>a</sup> Alq<sub>3</sub> assignments from ref 26 and graphitic carbon mode assignments based on refs 27 and 34.

and discussion of all peak fit modes is available in the Supporting Information.

Part b of Figure 1 shows the Alq<sub>3</sub> spectrum after deposition of 5 Å Mg and is dominated between 1200 and 1600 cm<sup>-1</sup> by modes attributable to graphitic carbon. Raman spectroscopy has been widely used to characterize different forms of graphitic carbon with high specificity and sensitivity, and its spectral features are well characterized.<sup>28</sup> These modes are especially intense with the 514.5 nm excitation used here due to resonant enhancement of the Raman scattering. Thus, given the intensities observed in these graphitic carbon bands, it is likely that only small amounts of graphitic carbon are produced. The broad mode centered at 1549 cm<sup>-1</sup> is known as the G-band and is a ring stretching mode of large sp<sup>2</sup> graphitic carbon domains. The broad mode at 1340 cm<sup>-1</sup> is assigned to the graphitic carbon D-band, a ring stretching mode due to sp<sup>3</sup> defect sites that are forbidden in perfect graphite; its presence in this spectrum indicates disorder in the graphitic carbon.<sup>27</sup> The known low-frequency asymmetry of both the G- and D-bands of graphitic carbon is fit using additional Gaussian bands at 1400 and 1200 cm<sup>-1</sup> respectively according to the procedure outlined by Ferrari and Robertson.<sup>27</sup> Additionally, a ring stretching mode of the D'-band and an overtone mode associated with the presence of polycrystalline graphite in small grains are observed at 1610 cm<sup>-1</sup>.<sup>27</sup> Lastly, a broadband at 560 cm<sup>-1</sup> corresponds to a weak out-of-plane vibrational mode of amorphous graphite, observed previously only in sp<sup>3</sup>-rich graphite.<sup>34</sup>

The ratio of peak intensities for the D-band to G-band fits is 0.5–0.6 for all Mg coverages between 5 and 20 Å, indicating the presence of amorphous or nanocrystalline graphite containing regions of both sp<sup>2</sup> and sp<sup>3</sup> character. The growth of the graphitic D- and G-band modes continues for deposition of 10 to 15 Å Mg. Finally, the intensity of all product modes decreases at 20 Å Mg mass thickness (Figure 2), indicating complete reaction of all available Alq<sub>3</sub> at the interface and the accumulation of metallic Mg clusters. The formation of this metallic Mg leads to attenuation of the electromagnetic field intensity with a

(34) Tamor, M. A.; Vassell, W. C. *J. Appl. Phys.* **1994**, *76*, 3823.

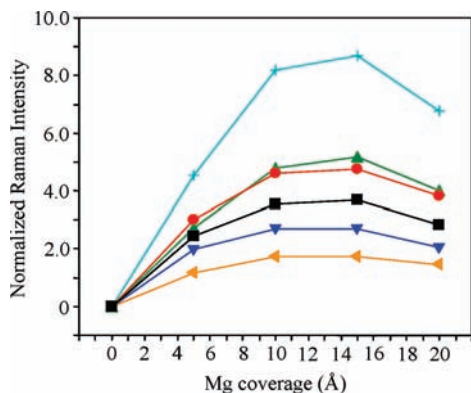


**Figure 2.** Normalized Raman intensity as function of metal coverage for Mg on Alq<sub>3</sub> for the graphite G-band at 1549 cm<sup>-1</sup> (+ light blue cross),  $\nu_{\text{ring}}$  at 1520 cm<sup>-1</sup> (• red circle),  $\nu_{\text{ring}}$  at 1354 cm<sup>-1</sup> (■ black square), graphite D-band at 1340 cm<sup>-1</sup> (▲ green triangle),  $\nu(\text{Mg}-\text{O})$  at 572 cm<sup>-1</sup> (▲ yellow triangle), and  $\nu(\text{Mg}-\text{C})$  at 420 cm<sup>-1</sup> (▽ blue triangle). All modes normalized to intensity of  $\nu_{\text{ring}}$  at 1394 cm<sup>-1</sup> of pristine Alq<sub>3</sub>.

concomitant reduction in Raman scattered intensity. A similar reduction in Raman signal was noted with deposition of  $\geq 20$  Å Ag and Al on Alq<sub>3</sub>.<sup>17,29</sup> Progressive conversion to graphitic carbon has also been reported for deposition of Al onto Alq<sub>3</sub><sup>17</sup> and C60 thin films<sup>35,36</sup> but has not been previously reported for the Mg–Alq<sub>3</sub> system.

The intense Alq<sub>3</sub> ring stretching modes at 1394 and 1595 cm<sup>-1</sup> shift to lower frequency by 5 cm<sup>-1</sup> upon deposition of 5 Å Mg (part b of Figure 1). Weaker modes present in the pristine Alq<sub>3</sub> film are no longer visible upon deposition of Mg due to the appearance of numerous, broad product modes. In XPS studies of the Mg–Alq<sub>3</sub> interface, Shen et al. observed a shift to lower binding energy by  $\sim 0.6$  eV for the C, N, and O 1s core levels upon deposition of 4 Å Mg.<sup>6</sup> This shift was attributed to alteration of the interface dipole upon deposition of Mg. Although a change in interface dipole is not necessarily expected to result in a frequency shift of the ring modes upon Mg deposition, a change in ring polarizability is possible with a commensurate change in Raman spectral intensity expected. It is proposed that these ring modes decrease in frequency due to formation of a Mg–Alq<sub>3</sub> adduct. The added mass of Mg bound to or near the 8-HQ ring system and/or a reduction in the electron density of the 8-HQ  $\pi$ -system due to back-bonding with Mg<sup>δ+</sup> could explain such a frequency decrease. The apparent absence of unreacted Alq<sub>3</sub> modes in the spectrum after deposition of 5 Å Mg suggests formation of an interfacial product along with an interface dipole as reported by Shen et al.<sup>6</sup> This interface dipole could lead to an increase in overall polarizability of molecular species at the interface, resulting in an increase in Raman scattering intensity. In fact, a slight intensity enhancement for species in the vicinity of the deposited Mg is suggested by comparison of the Mg–Alq<sub>3</sub> and graphitic carbon product mode intensities in parts b–e of Figure 1 with those of the pristine Alq<sub>3</sub> film in part a of Figure 1.

In recent theoretical studies, Meloni et al. proposed a stable 2:1 complex of Alq<sub>3</sub>–Mg in which Mg is bound to the 8-HQ ring system of one Alq<sub>3</sub> through one O atom and two C atoms with further coordination with an O atom on a neighboring Alq<sub>3</sub>

molecule.<sup>13,14</sup> This structure is wholly consistent with the  $\nu_{\text{ring}}$  frequency shifts observed here. Bond formation between Mg and a 8-HQ C atom is further supported by the observation of a  $\nu(\text{Mg}-\text{C})$  mode at 420 cm<sup>-1</sup> for the Mg–Alq<sub>3</sub> complex. The region from 200 to 500 cm<sup>-1</sup> is free of intense Raman-active modes for Alq<sub>3</sub>,<sup>26</sup> indicating that modes observed in this window upon deposition of Mg must be due to Mg–Alq<sub>3</sub> bonding. The assignment of the band at 420 cm<sup>-1</sup> has as precedent the previous observation of  $\nu(\text{Mg}-\text{C})$  modes in a similar spectral region. For example,  $\nu(\text{Mg}-\text{C})$  modes for diethylmagnesium have been observed at 350, 383, and 468 cm<sup>-1</sup>,<sup>37</sup> similarly,  $\nu(\text{Mg}-\text{C})$  modes at 233 and 461 cm<sup>-1</sup> have been reported for bis(cyclopentadienyl) magnesium.<sup>23</sup> The shift in the  $\nu_{\text{ring}}$  modes to lower frequencies further supports assignment of the 420 cm<sup>-1</sup> band to the  $\nu(\text{Mg}-\text{C})$ . As previously noted,<sup>17</sup> such a frequency decrease is consistent with back-bonding of  $\pi$ -electrons in the 8-HQ ligand to the deposited Mg atom.

A number of additional modes not observed in the pristine Alq<sub>3</sub> film also appear upon deposition of 5 Å Mg. A new band appears at 1070 cm<sup>-1</sup> that is assigned as a  $\nu(\text{C}-\text{O})$  mode. This mode is likely down-shifted from the [ $\nu(\text{C}-\text{O}) + \delta(\text{C}-\text{H})$ ] combination mode of Alq<sub>3</sub> at 1117 cm<sup>-1</sup> due to a reduction in electron density on the O atom upon bonding of its lone-pair electrons to the Mg adatom. Two new  $\nu(\text{C}-\text{N})$  modes at 1205 and 1218 cm<sup>-1</sup> also appear in part b of Figure 1, shifted from 1230 cm<sup>-1</sup> for pristine Alq<sub>3</sub>. The presence of two bands is suggestive of two chemically distinct C–N bonds in the Mg–Alq<sub>3</sub> complex. As with the  $\nu_{\text{ring}}$  modes, the shift to lower frequency of the  $\nu(\text{C}-\text{N})$  modes can be attributed to reduction in electron density of the pyridyl ring upon Mg binding to a C atom in the 8-HQ ligand, with the 1205 cm<sup>-1</sup> band shifting further due to the increase in reduced mass from the bonded Mg.

The appearance of two distinct  $\nu(\text{C}-\text{N})$  modes, the appearance of a  $\nu(\text{Mg}-\text{C})$  mode, and shifts in the 8-HQ  $\nu_{\text{ring}}$  modes discussed above all support formation of a Mg–Alq<sub>3</sub> complex in which Mg is bound to the pyridyl ring of the 8-HQ ligand through the C atom adjacent to the N atom as depicted in Figure 3 for possible 1:1 and 1:2 Mg–Alq<sub>3</sub> complexes. Further evidence for interaction of at least one pyridyl ring with the Mg is the frequency increase of the  $\nu(\text{Al}-\text{N})$  from 918 to 999 cm<sup>-1</sup>.<sup>29</sup> This shift is rationalized as a strengthening of the Al–N bond due to shifting electron density from the central Al toward the ligand as a result of Mg insertion, thereby shortening and strengthening the Al–N bond. This explanation is supported by the XPS observations of Shen et al. in which the N 1s core level shifts to lower binding energy upon Mg deposition, consistent with an increase in electron density on the N.<sup>6</sup>

The broad mode at 614 cm<sup>-1</sup> observed in parts b–e of Figure 1 upon deposition of Mg thicknesses between 5 and 20 Å is assigned to the  $\nu(\text{Mg}-\text{O})$  of the Mg–Alq<sub>3</sub> adduct. This assignment is supported by the XPS observations of Shen et al. of a shift to higher binding energy of the O 1s by 1.4 eV, consistent with a decrease in electron density on the O atom upon bonding of the lone-pair electrons to the inserted Mg.<sup>6</sup>

Significantly, formation of the Mg–O bond, shortening of the Al–N bond, and lengthening of the Al–O bond in the Mg–Alq<sub>3</sub> adduct are all predicted in DFT calculations for the lowest-energy product for reaction of Mg with *mer*-Alq<sub>3</sub>.<sup>13,14</sup> The structure for the Mg–Alq<sub>3</sub> adduct proposed by Meloni et al. on the basis of DFT calculations places the inserted Mg in

(35) Hebard, A. F.; Eom, C. B.; Iwasa, Y.; Lyons, K. B.; Thomas, G. A.; Rapkine, D. H.; Fleming, R. M.; Haddon, R. C.; Phillips, J. M.; Marshall, J. H.; Eick, R. H. *Phys. Rev. B* **1994**, *50*, 17740.

(36) Khalid, F. A.; Beffort, O.; Klotz, U. E.; Keller, B. A.; Gasser, P.; Vaucher, S. *Acta Materialia* **2003**, *51*, 4575.

(37) Kress, J.; Novak, A. *J. Organomet. Chem.* **1976**, *121*, 7.

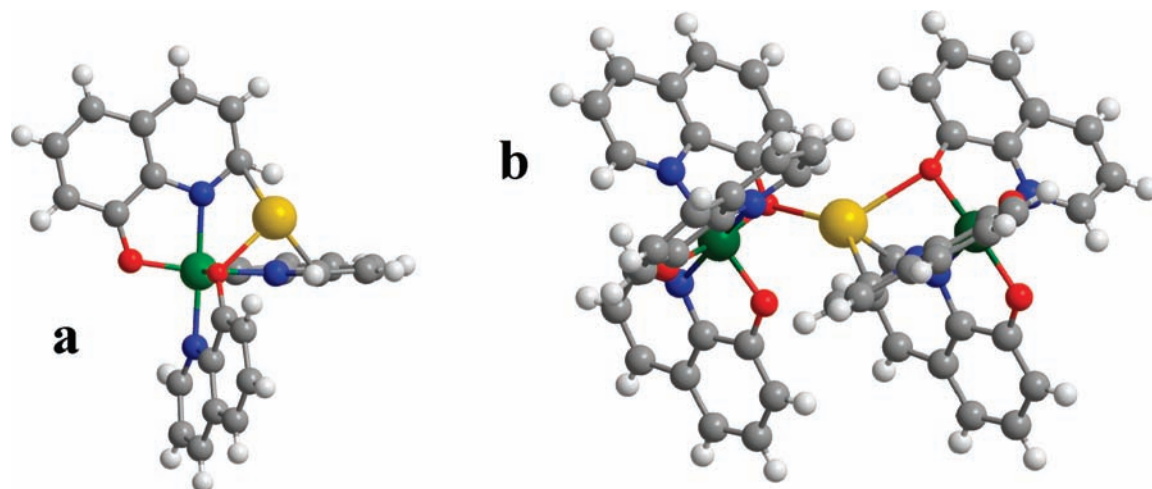


**Figure 3.** a) Proposed Mg–Alq<sub>3</sub> adduct with Mg bonded to the 8-HQ O atom and the C atom of the 8-HQ pyridine ring; b) Mg(Alq<sub>3</sub>)<sub>2</sub> adduct with Mg bound to two Alq<sub>3</sub> through the 8-HQ O and C atoms. C (gray), H (white), N (blue), O (red), Al (green), and Mg (yellow).

between neighboring Alq<sub>3</sub>, with Mg bound to the O atom of one Alq<sub>3</sub> and two C atoms and one O atom of the other Alq<sub>3</sub>. Such a structure is completely consistent with all Raman spectral observations and assignments reported here.

Many of the changes observed in the Alq<sub>3</sub> Raman spectral and XPS responses upon Mg deposition are similar to those observed previously in studies of the Al/Alq<sub>3</sub> system.<sup>6</sup> Studies of the Al–Alq<sub>3</sub> interaction by DFT calculations,<sup>9,11,15</sup> XPS,<sup>3,4,8</sup> and Raman spectroscopy<sup>17</sup> indicate an Al–Alq<sub>3</sub> complex with Al bound through the O atom of the 8-HQ ligand. On the basis of shifts in the  $\nu(\text{C–O})$ ,  $\nu(\text{C–N})$ , and  $\nu_{\text{ring}}$  modes and the appearance of new  $\nu(\text{Mg–C})$  and  $\nu(\text{Mg–O})$  modes, a structure for the Mg–Alq<sub>3</sub> adduct is proposed in Figure 3 in which Mg is bound through both the O and C atoms of *mer*-Alq<sub>3</sub>. In addition, changes to the C, N, and O 1s core levels for Mg on Alq<sub>3</sub> are identical to those observed for the Al–Alq<sub>3</sub> system,<sup>6</sup> suggesting a structurally related metal–Alq<sub>3</sub> adduct in both systems. Despite these similarities, the Raman spectral response for the Mg–Alq<sub>3</sub> system is significantly different in several key ways from that for the Al–Alq<sub>3</sub> system for similar mass thicknesses of metal.<sup>17</sup> Specifically, a new band at 420 cm<sup>−1</sup> due to the  $\nu(\text{Mg–C})$  mode is observed in the Mg–Alq<sub>3</sub> system but not the Al–Alq<sub>3</sub> system. Additionally, splitting of the  $\nu(\text{C–N})$  as a result of Mg binding to the 8-HQ pyridyl ring is observed for the Mg–Alq<sub>3</sub> system, whereas no similar splitting is observed in the Al–Alq<sub>3</sub> system.

It is interesting to note that, on the basis of the Mg atomic ionization potential<sup>38</sup> and the Alq<sub>3</sub> electron affinity,<sup>39</sup> electron transfer from Mg to Alq<sub>3</sub> is predicted. However, no spectral evidence for formation of the simple Alq<sub>3</sub> anion radical is observed upon deposition of Mg between 5 and 20 Å mass thicknesses. The presence of additional electron density in the 8-HQ<sup>−•</sup>  $\pi$ -system might be expected to shift the  $\nu_{\text{ring}}$  at 1595 cm<sup>−1</sup> and the  $\nu(\text{C–N})$  at 1230 cm<sup>−1</sup> to higher frequency. In fact, shifts in the opposite direction are actually observed, consistent with a decrease in ring electron density. This behavior

suggests that a simple charge transfer model is insufficient to explain the interaction between Mg and Alq<sub>3</sub> in the solid-state interface.

Moreover, as shown in Figure 2, intensities of the  $\nu_{\text{ring}}$  modes at 1585 and 1383 cm<sup>−1</sup> and that of the  $\nu(\text{Mg–C})$  at 420 cm<sup>−1</sup> for the Mg–Alq<sub>3</sub> adduct remain relatively constant after deposition of 10 Å Mg up to the maximum Mg thickness studied of 20 Å. This saturation of the Mg–Alq<sub>3</sub> modes with only 10 Å Mg is consistent with a substantial reaction that rapidly converts the uppermost layers of Alq<sub>3</sub> in the film. Deposition of additional Mg beyond a mass thickness of  $\sim 10$  Å only furthers decomposition of the thin film to graphitic carbon, most likely through reduction of the Mg–Alq<sub>3</sub> adduct by excess Mg. The reactivity of the 1:1 and 1:2 Mg–Alq<sub>3</sub> adducts upon deposition of excess Mg has yet to be investigated; however, these results suggest that electron transfer from excess Mg to the metal–Alq<sub>3</sub> adducts may be possible. The lack of additional Mg–C and Mg–O bonding at Mg coverages  $>10$  Å in this investigation, however, indicates that additional electron transfer from Mg to the Mg–Alq<sub>3</sub> adduct does not lead to the formation of stable metal–organic species but may lead to formation of organic radical species that may catalyze further degradation at the interface. Further work is needed to develop a detailed understanding of the electronic properties of the proposed Mg–Alq<sub>3</sub> adducts and to assess their potential reactivity with excess Mg atoms. Work is underway in this laboratory to access the effect of thin insulating layers such as LiF on the reactivity at interfaces such as Mg/Alq<sub>3</sub> in hopes of further elucidating the factors influencing the formation of metal–Alq<sub>3</sub> adducts and graphitic carbon.

It should be noted that the Alq<sub>3</sub> films were held at 90 K during Mg deposition in this study to ensure a high sticking coefficient for Mg. This temperature is considerably lower than the room-temperature construction of real organic electronic devices from these materials. Although this temperature is not believed to significantly alter the structures of either the Alq<sub>3</sub> film or its reaction products, cooling of the samples may result in reduced diffusion of the deposited Mg, thereby limiting the reaction depth and creating a narrower metal–organic interfacial region than formed in real devices. Raman spectra of a 150 Å Alq<sub>3</sub> film topped by 5 Å of Mg as a function of temperature are available in the Supporting Information. These spectra confirm

(38) *CRC Handbook of Chemistry and Physics*, 64th ed.; Weast, R. C., Ed.; CRC Press: Boca Raton, FL, 1984.

(39) Schlaf, R.; Parkinson, B. A.; Lee, P. A.; Nebesny, K. W.; Jabbour, G.; Kippelen, B.; Peyghambarian, N.; Armstrong, N. R. *J. Appl. Phys.* **1998**, *84*, 6729–6736.

that few structural changes are observed upon heating the Mg–Alq<sub>3</sub> film from 100 to 300 K. However, to completely understand the nature of the interaction of Mg with Alq<sub>3</sub>, further experimental work is needed in which the reaction of Mg with simple organic constituent parts of Alq<sub>3</sub> is characterized. These studies are currently underway in this laboratory and will be reported at a later date.

### Conclusions

Raman spectra of Alq<sub>3</sub> films exhibit significant spectral changes upon deposition of 5 to 20 Å Mg. The loss in intensity of all major Alq<sub>3</sub> modes coupled with the appearance of new modes support the partial reactive conversion of Alq<sub>3</sub> to a new product in which Mg is bound to Alq<sub>3</sub> through the O atom and C atoms of 8-HQ. The observed shifts in  $\nu_{\text{ring}}$ ,  $\nu(\text{C}-\text{N})$ ,  $\nu(\text{Al}-\text{N})$ , and  $\nu(\text{Al}-\text{O})$  along with appearance of  $\nu(\text{Mg}-\text{O})$  and  $\nu(\text{Mg}-\text{C})$  modes support the Mg–Alq<sub>3</sub> adduct structure suggested by Meloni based on theoretical investigations.<sup>13,14</sup> The formation of this Mg–Alq<sub>3</sub> adduct is further supported by XPS studies detailing the electronic consequences of the interaction of Mg with Alq<sub>3</sub>.<sup>6</sup>

The appearance and growth of graphitic carbon modes at 1610, 1549, 1400, 1340, 1200, and 540 cm<sup>-1</sup> indicate a degradation pathway for the conversion of Alq<sub>3</sub> to graphitic carbon after the deposition of Mg, which may result from the interaction of excess Mg atoms in the interfacial region with the Mg–Alq<sub>3</sub> adduct. Both the frequency and the relative ratio of the D-Band and G-Band graphitic modes observed at the Mg–Alq<sub>3</sub> interface indicate small grain, nanocrystalline, or amorphous graphite is formed as a result of partial decomposition of the organic film.<sup>27</sup> Graphitic carbon has a Raman cross-section that is 1 to 2 orders of magnitude greater than that for simple organic molecules; thus, the observed graphite is likely to be present in small amounts at this interface. Nonetheless, the amount of graphitic carbon produced in this system is significantly higher than that observed for the Al/Alq<sub>3</sub> system at comparable coverages illustrating important chemical differences in reactive Alq<sub>3</sub> interfaces with seemingly similar metals. Such differences could account for the observed differences in electron transfer across these interfaces.

The presence of both the Mg–Alq<sub>3</sub> adduct reaction product and graphitic carbon at this interface may have profound implications for electron transport in real devices. Formation of a Mg–Alq<sub>3</sub> complex at the interface may have several effects on charge injection. As supported by previous UPS work,<sup>5–7,10</sup> the Mg–Alq<sub>3</sub> complex is likely to have an energy level in the gap between the LUMO of the bulk Alq<sub>3</sub> film and the Mg Fermi level. Graphitic carbon could also possess energy states in this gap region because its work function is known to be lower than that of Mg<sup>40</sup> and subject to mediation by the presence of metallic impurities.<sup>41</sup> These gap states could serve as intermediate states for electron injection from the metal Fermi level to the Alq<sub>3</sub> LUMO, thereby lowering the energy required for this process.<sup>42,43</sup> The presence of both reaction products and decomposition products is also likely to create disorder within the interface that would further broaden interfacial state energies and lower the energy required for electron injection.

The reactive conversion of Alq<sub>3</sub> to an adduct species with low Mg coverage, along with partial graphitization of the film at all Mg coverages, indicate a more chemically complex and varied interfacial region than previously reported for Mg–Alq<sub>3</sub>. The spectral changes observed for the Mg/Alq<sub>3</sub> system speak to the power of surface Raman spectroscopy for molecular characterization of such metal–organic interfaces.

**Acknowledgment.** The authors gratefully acknowledge support of this research by the National Science Foundation.

**Supporting Information Available:** Complete listing of bands peak fit in the spectral data shown in Figure 1, along with their assignments and supporting discussion. This material is available free of charge via the Internet at <http://pubs.acs.org>.

JA808021D

(40) Obratsova, A. N.; Volkova, A. P.; Boroninc, A. I.; Kosheev, S. V. *Diamond Relat. Mater.* **2002**, *11*, 813–818.

(41) Kyas, A.; Fleischhauer, J.; Steinmetz, E.; Wilhelmi, H. *Plasma Chem. Plasma Proc.* **1993**, *13*, 223–235.

(42) Bulovic, V.; Tian, P.; Burrows, Gokhale, M. R.; Forrest, S. R. *Appl. Phys. Lett.* **1997**, *70*, 2954.

(43) Baldo, M. A.; Forrest, S. R. *Phys. Rev. B* **2001**, *64*, 85201.